Experimental and theoretical study of iron concentration on clogging phenomenon in secondary circuit of pressurized nuclear power plant

T. Muller[a], A. Mourgues[a,*], F. Pedler[c], A. Lassauce[a], M. Guillodo[a], P. Dolleans[a], M. Caron-Charles[b]

[a] Technical Center, AREVA NP, 30 bd de l'Industrie – 71200 Le Creusot

[b] Research & Development Department AREVA, Tour AREVA – 1 Place Jean Millier, 92084 Paris.

[c] Engineering & Projects, AREVA NP, Tour AREVA – 1 Place Jean Millier, 92084 Paris.

* e-mail: alejandro.mourgues@areva.com

ABSTRACT

The clogging phenomenon can be observed in both primary and secondary circuits of a Pressurized Nuclear Power Plant (PWR). This effect is associated to hydrodynamic singularity produced by an important change in flow velocity (e.g. SG tube' support plates) and physico-chemical conditions. In Steam Generator (SG) secondary side the thickness of the clogging can become so important that the performance could be reduced. Two experimental tests were carried out to study the evolution of the clogging on a specimen (important section flow reduction) in single phase conditions of secondary circuit (245 – 275°C, 10 MPa) with low (5 to 9.5 ppb) and high (5 to 27 ppb) iron concentration for 760 and 470 hours respectively. To increase the deposits kinetics, the velocities were set between 5 to 30 m/s. The deposit mean thickness change was calculated by the evolution of the pressure drop coefficient assuming deposit profile and geometry measured at the end of the tests. Moreover, a model based on Graetz mass transfers has been used to estimate the kinetics of deposit formation. The results showed that experimental and model results are in good agreement. It suggests that the clogging effect in our experimental conditions is controlled by mass transfer and not by the electro-kinetic effect. However, the electro-kinetic effect would provide the conditions to initiate the deposit formation.

The model was implemented in the CLOSIS program (developed by AREVA) to simulate the clogging effect in a steam generator. Theoretical estimations are in good agreement with SG on-site measurement and this for 20 years experience feedback.

Keywords: Clogging effect, streaming current, mass transfer, steam generator, pressure drop.

1. Introduction

Different deposit formations can be observed in the primary as in secondary circuit of a Steam Generator (SG) from a nuclear power plant (e.g. fouling and clogging). When the thickness of the deposit becomes too important, the efficiency of the steam generator (SG) can be reduced. Thus, the prediction of the deposition kinetics and physico-chemical conditions for which it can be formed, gives important information to optimize the SG operation, to minimize the risk of deposition and estimate the performances on the time.

In SG, three deposit phenomena can be identified [1][2]: fouling, clogging and spalling. Fouling is related to the accumulation of unwanted "materials" on interface metal/solution to the detriment of the function (i.e. heat transfer). It can be formed by corrosion, chemical reaction, solubility, precipitation, etc. [3]. Clogging is related to the deposit of unwanted materials on interface metal/solution due to stream currents [3][4][5]. The deposit is formed and fills up the interstices, in particular the TSP openings, preventing the normal flow distribution. The different deposit layers, as flake shape in our case, can take off from SG tubes and fill up the different cavities as the tetra-foil opening of the TSP [2]. This phenomenon is called spalling.

Different models try to predict the deposit phenomena: C. Henry et al. [6] focus the study on fouling effect [6], S. Girard et al. [7] carried out a statistical analysis on the different parameters on SG clogging effect, but no phenomenological model was formulated. T. Prusek [2] proposed a model based on flashing phenomenon, where it was obtained good agreement with experimental results. At the difference of T. Prusek results, in our experimental conditions, flashing is not possible, however it was observed clogging effect. It shows that there are others phenomena at the origin of the clogging.

This work is focused on the clogging phenomenon. The formation kinetics depends of the operating conditions (velocity flow, T, P) and water characteristics (hydrogen, Fe and colloid concentration, pH, etc). Here, a macroscopic model based on mass transfer has been proposed. The model predictions are compared with experimental data at similar SG temperature and pressure conditions and with SG on-site feedback data.

Figure 1 shows a diagram of the steam generator of a Pressurized Water Reactor (PWR) power plant. Hot water coming from nuclear reactor (primary circuit) flows into the tubes of the steam generator. In the other side of the tubes, the vapor is produced (secondary circuit). The tubes are fixed along the steam generator vessel by several TSPs whose geometries change in function of the steam generator design. Figure 1 shows a tetrafoil opening.

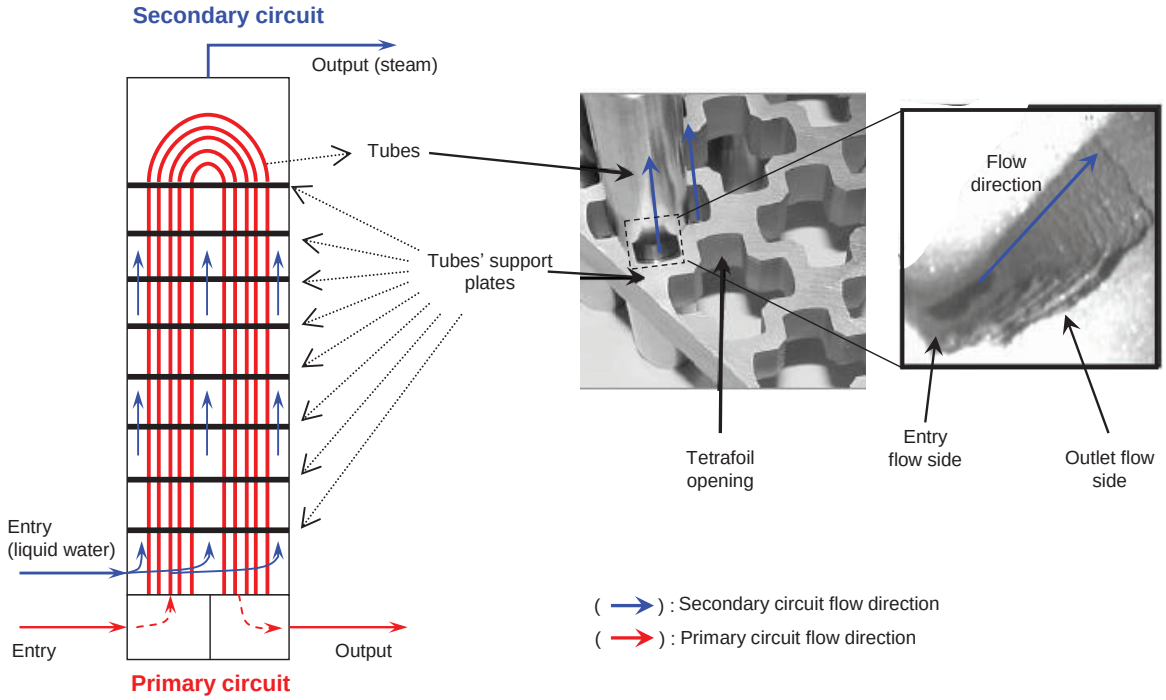

Figure 1 – Diagram of steam generator device and tube support plate

On right side of Figure 1 we can notice a real clogging effect on a tetrafoil opening of a TSP. The entry flow side of the opening is more filled up compared to the outlet flow side. Moreover, rolls-deposit are formed over the entire length. As it will be shown later, similar deposit shapes were obtained in our experimental loop.

2. Experimental loop

The Figure 2 shows the experimental loop. It consists essentially of a specimen (sudden constriction), a by-pass circuit and a water chemical conditioning unit.

The specimen produces an important change in flow velocity, predisposing the clogging effect ([3]-[10]). It is made (see Figure 3) of a convergent cone-shaped section at the entry followed by a first cylindrical section (4.21 mm in diameter, S2), a second cylindrical section (2.9 mm in diameter and 10 mm long, S3) with abrupt cross-section changes, a third cylindrical section (4.21 mm in diameter, S4) and finally a divergent cone-shaped section. The clogging phenomenon was observed in the smallest specimen cross section (S3), principally at the inlet leading to an additional restricted section Sc.

The by-pass circuit enables to keep the pressure and temperature constant during the tests. It consists of an electrical heating system and a pump. The pressure is kept constant by a forced feeding pump (no showed on Figure 2). The flow rate in the circuit depends on the clogging conditions in the specimen. The volumetric flow rate is measured by three different flow meters (two venturis and one diaphragm) and the pressure drop through the specimen is measured by a pressure transducer. A second electrical heating system upstream of the specimen allows to better control the temperature conditions.

The water chemical conditioning unit is used for on-line measurement and control of the chemical conditions in the loop, such as pH, conductivity and iron concentration (by ICP-AES and ICP-MA analysis).

In order to observe the clogging phenomena with reasonable test duration, the flow velocity through specimen is much higher compared to real conditions (between 5 to 30 m/s compared to ~1 m/s in SG conditions).

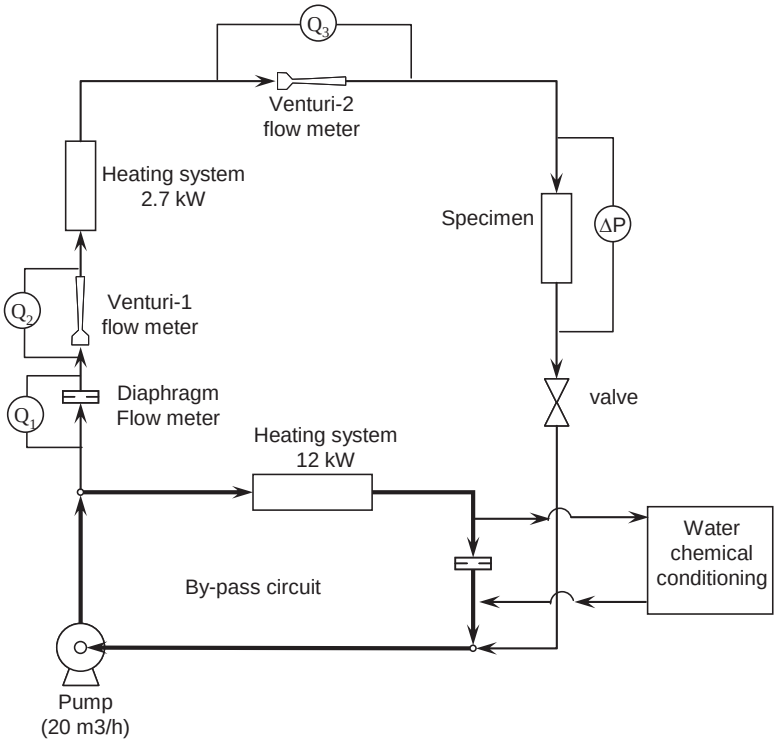

Figure 2 – Experimental loop

3. Modeling

In our experimental tests, we measure the change in pressure drop through the specimen, iron concentration and volumetric flow during the test. On the basis of the deposit shape (observed at the end of previous tests) we can assume a suitable geometric coating shape to calculate the pressure drop coefficient, and by this way, estimate the mean increase (growth) in deposit thickness and the flow velocity through the specimen (see Figure 3). With these data we can directly obtain the experimental kinetics of the deposit layer growth rate: change in $(de/dt)_{\exp}$.

Figure 3 shows the equations used to calculate the pressure drop through the specimen. As will be shown below, typically a ring of deposit is formed at the entrance of the sample. Its pressure drop is calculated by the coefficient K_{BC} (see Figure 3) where the height of deposit (e) deduced from overall measured pressure drop.

According to equation (3), the deposit geometry may be modeled as a cylindrical ring shape section similar to experimental profile observed. However, as will be shown below (section 4.1.2), at high concentration the shape and geometry of the deposit changes during the test. These changing were considered in the model.

From experimental data S_C is estimated as time function. Then:

$$S_C(t) = \frac{\pi}{4} D_C^2 \tag{1}$$

$$D_C(t) = D_3 + 2 \cdot e(t) \tag{2}$$

$$\frac{dS_C(t)}{dt} = \pi \cdot (D_3 + 2 \cdot e(t)) \cdot \frac{de(t)}{dt} \tag{3}$$

Where l_C is obtained from thickness profile measurement after test.

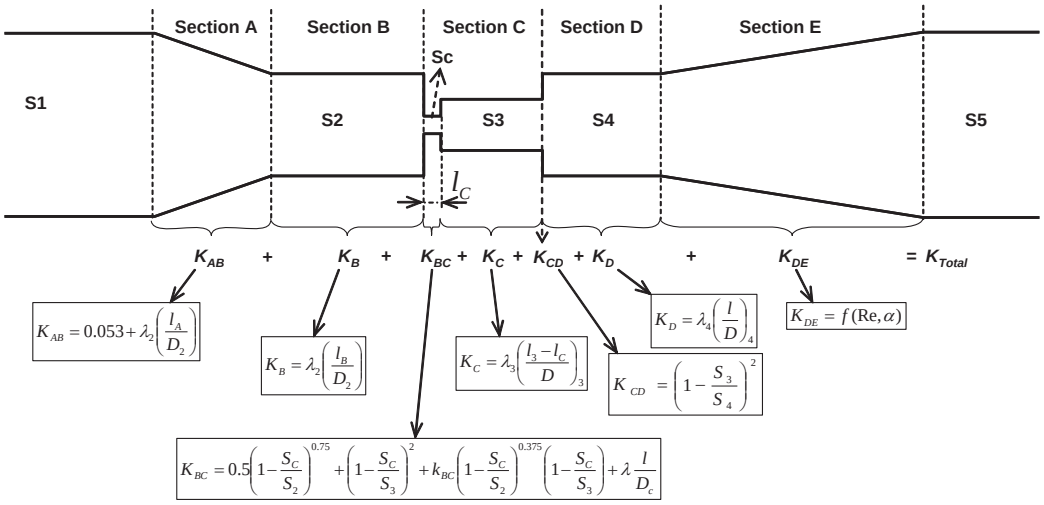

Figure 3 – Diagram showing specimen and equation of pressure drop coefficients [11]

On the other hand, as we know how the flow velocity develops, we can estimate the mass transfer coefficient using appropriate mass transfer correlations. Finally, from these calculations we can obtain the theoretical kinetics of the deposit layer growth rate $(de/dt)_{cal}$ (theoretical change).

If both the changes in (de/dt) (from pressure drop and estimations from mass transfer) and the order of magnitude are similar, we can conclude that the mechanism that controls the deposit evolution is the mass transfer and the electrokinetic effect (much faster) can be ignored when describing the deposit thickness growth rate. Nevertheless the flow velocity and the chemical conditions must be adequate to activate the electrokinetic effect, which is the condition to initiate the deposit phenomena [4][5].

The deposit kinetics can be modelled like:

$$\frac{dm}{dt} = k_m \cdot (C_{Fe,bulk} - C_{Fe\,\mathrm{interface}}) \cdot S(t) \tag{4}$$

Where:

$$m(t) = \rho \cdot (1 - \varepsilon) \cdot S(t) \cdot e(t) \tag{5}$$

If we consider that the density and porosity of the deposit are constant during the test,

$$\frac{de(t)}{dt} = \frac{k_m \cdot (C_{Fe,bulk} - C_{Fe\,\mathrm{interface}})}{\rho \cdot (1 - \varepsilon)} - \frac{e(t)}{S(t)} \cdot \frac{dS(t)}{dt} \tag{6}$$

Our calculations showed that the second term of equation (3) can be negligible, thus we obtain the following equation which describes the kinetics of the deposit thickness growth.

$$\frac{de}{dt} = \frac{k_m \cdot (C_{Fe\,bulk} - C_{Fe\,interface})}{\rho \cdot (1-\varepsilon)} \tag{7}$$

If the kinetic "reaction" producing the clogging on the surface is much faster that mass transfer, it can be assumed that the iron concentration at the interface is negligible compared to bulk concentration, so $C_{Fe\,interface} = 0$.

The following equations were used to estimate the mass transfer coefficient and are directly written with dimensionless numbers. In our calculations, we consider two boundary layer zones: a developing boundary layer (just at the entry of the specimen) and a fully developed boundary layer.

- *Mass transfer coefficient in the developing boundary layer.*

R.H. Notter and C.A. Sleicher propose a numerical solution for the Graetz problem in turbulent conditions [13][14]. This solution is valid for a wide range of Re and Pr numbers. For a Pr = 0.72 (near to our conditions) and heat transfer with a constant wall temperature:

$$Sh_x = \frac{k_{m,x} \cdot D}{D_{m,ij}} = \frac{\sum_{n=0}^{n=\infty} A_n \cdot e^{-\lambda_n^2 x}}{2 \cdot \sum_{n=0}^{n=\infty} \frac{A_n}{\lambda_n^2} \cdot e^{-\lambda_n^2 x}} \tag{8}$$

$$x = \frac{2 \cdot X}{\mathrm{Re} \cdot Sc \cdot D} \tag{9}$$

$$\lambda_n = \left(n + \frac{2}{3} \right) \Big/ G \tag{10}$$

$$k = G \cdot \lambda_n \text{ for n > 2} \tag{11}$$

$$A_n = \frac{0.201}{G} \cdot \left(\frac{H}{\lambda_n} \right)^{1/3} \cdot \left[1 - \frac{1}{k^2} \left(\frac{c}{2\pi} \left(Ln(k \cdot \pi) - 1 \right) + \frac{7}{36\pi^2} \right) \right] \tag{12}$$

$$H = \frac{\mathrm{Re} \cdot \lambda}{32} \tag{13}$$

Where $G = f(\mathrm{Re}, \mathrm{Pr})$[13].

- *Mass transfer in the fully developed boundary layer:*

We used the Petukhov, Kirilov and Popov correlation ($0.5 < Sc < 2000$, $10^4 < \mathrm{Re}_D < 5 \cdot 10^6$) [13][14]:

$$Sh_D = \frac{(f/8) \cdot \mathrm{Re}_D \cdot Sc}{1.07 + 12.7 \cdot (f/8)^{1/2} \cdot (Sc^{2/3} - 1)} \tag{14}$$

Where the friction factor (f) is obtained from the Moody diagram for smooth tubes by:

$$f = (1.82 \cdot Log_{10}(\mathrm{Re}_D) - 1.64)^{-2} \tag{15}$$

Where:

$$Sh = \frac{k_m \cdot D}{D_{m,ij}} \tag{16}$$

$$Sc = \frac{\mu}{\rho \cdot D_{m,ij}} \tag{17}$$

The molecular diffusion can be estimated by the Stokes-Einstein equation [12]:

$$D_{m,Fe-H2O} = \frac{k_B \cdot T}{6\pi \cdot \mu \cdot r} \tag{18}$$

The growth deposit is obtained injecting the mass transfer coefficients (obtained from equations 8 and 14) in equation 7.

The mass transfer model was validated by naphthalene sublimation test. The results are not showed here, but we obtained a good agreement of the Graetz formulation for our deposit profile.

4. Results and discussions

Two levels of iron concentrations were tested and we obtain similar experimental results (5 to 10 ppb and 5 to 27 ppb). In this paper, only experimental results of the test with iron concentration between 5 to 10 ppb will be presented on Figure 4.

Figure 4a shows the pressure drop and change in flow velocity through the specimen during the test. Figure 4b shows the normalized pressure drop coefficient (K / K_0), and iron concentration during the test. As we can see in Figure 4b, the iron concentration varies between 5.1 and 9.5 ppb during the test. These fluctuations were considered when estimating the mass transfer flux (equations 1 and 4).

On Figure 4b we can observe that the normalized pressure drop coefficient (resulting from clogging) increases regularly until around 168 hours of test. After that, regular growth and destruction of the deposit are observed. Indeed, part of the deposit is broken down and removed due to flow shearing, resulting in an abrupt and sizeable decrease in the K / K_0 values. In addition, as the flow cross-section increases when the deposit is removed, the flow velocity through the specimen decreases (see Figure 4a). This behaviour also depends on the chemical conditions of the water (pH, hydrogen and iron concentration, etc.).

For this test, after three hundred and eighty hours, the loop temperature was changed from 245°C to 275°C. It seems that in these conditions, the deposit kinetics is modified; nevertheless the deposit continues to be destroyed due to the flow shear effect.

After five hundred hours, the test loop valve was adjusted to reduce the flow velocity and observe the deposit kinetics at a lower value of around 5 m/s (see Figures 4a and b). In these conditions, we can see that the flow velocity and pressure drop decrease simultaneously which was not the case previously (see Figure 4a). Indeed, we noticed a clogging effect on the valve. This problem did not affect our analysis of deposit development because, the pressure drop is measured in the specimen section, and on the other hand, the flow measurements made by both the venturi and diaphragm flow-meters were in good accordance.

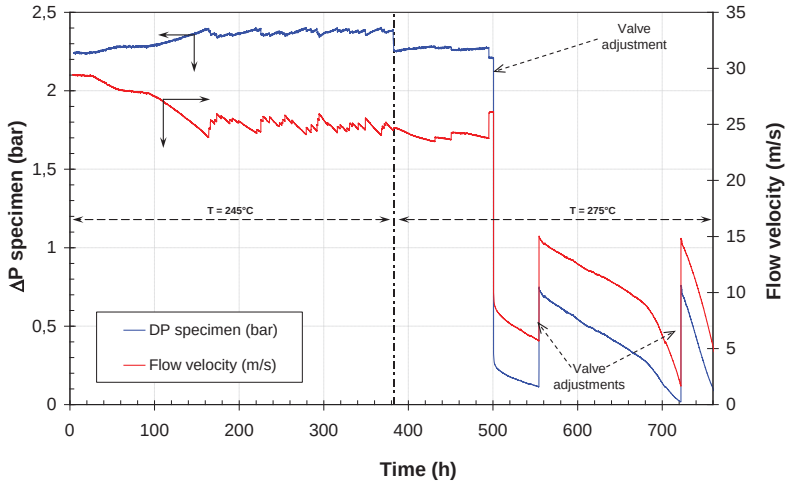

(a) Pressure drop and flow velocity through the specimen

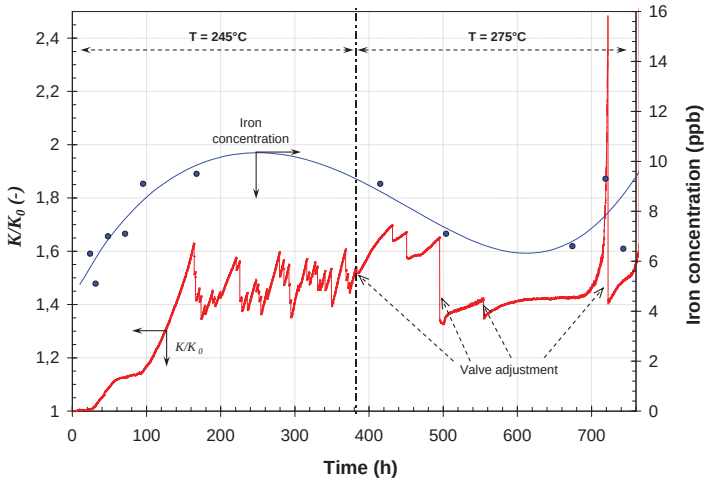

(b) Normalized pressure drop coefficient and iron concentration

Figure 4 – Pressure drop, iron concentration and flow velocity vs. test duration (low iron concentration (5 to 9.5 ppb) at 245 and 275°C)

Finally, no deposit breakdown was observed, probably because of the lower flow velocity after 500 h (resulting in a lower flow shearing effect).

Figure 5 shows the deposit profile measured after 760 hours test. As observed on Figure 5, the deposit is formed essentially at the specimen entry (80 µm high and 200 µm wide), probably due to the stronger effect of the streaming currents in this singularity; the mass transfer rate is higher here because the boundary layer is developed. In addition, roll-deposits were formed over the entire length of the specimen. In this case, our calculations showed that the most important pressure drop along the length of the specimen is due to the deposit formed at the entry of the specimen and that the roll-deposit can be ignored.

Figure 6 shows the change in the average thickness of the deposit estimated from pressure drop data. We can see that the model shows an acceptable prediction of the deposit thickness at the end of the

test. Indeed, the model prediction value and the measured value are 115 µm and 80 µm respectively. This difference can be partially explained by the breakdown and/or partial dissolution of the deposit during draining of the experimental loop.

Similar results were obtained for the test at high iron concentration (5 to 27 ppb). In this case the average deposit reaches a thickness of 570 µm and a width of 600 µm at the specimen inlet where the model calculated 470 µm. This results show, as expected, that iron concentration increase the kinetic deposition.

Figure 7 shows the change in (de/dt) as a function of flow velocity in the specimen for both experimental and theoretical estimations. We can observe that theoretical estimations are in agreement with experimental data. Indeed, the mass transfer velocity calculations are of same order of magnitude as the experimental data. These results suggest that the clogging effect in our experimental conditions is controlled by the mass transfer, and the electrokinetic effect is a faster phenomenon compared to mass transfer and then it can be ignored on model formulation.

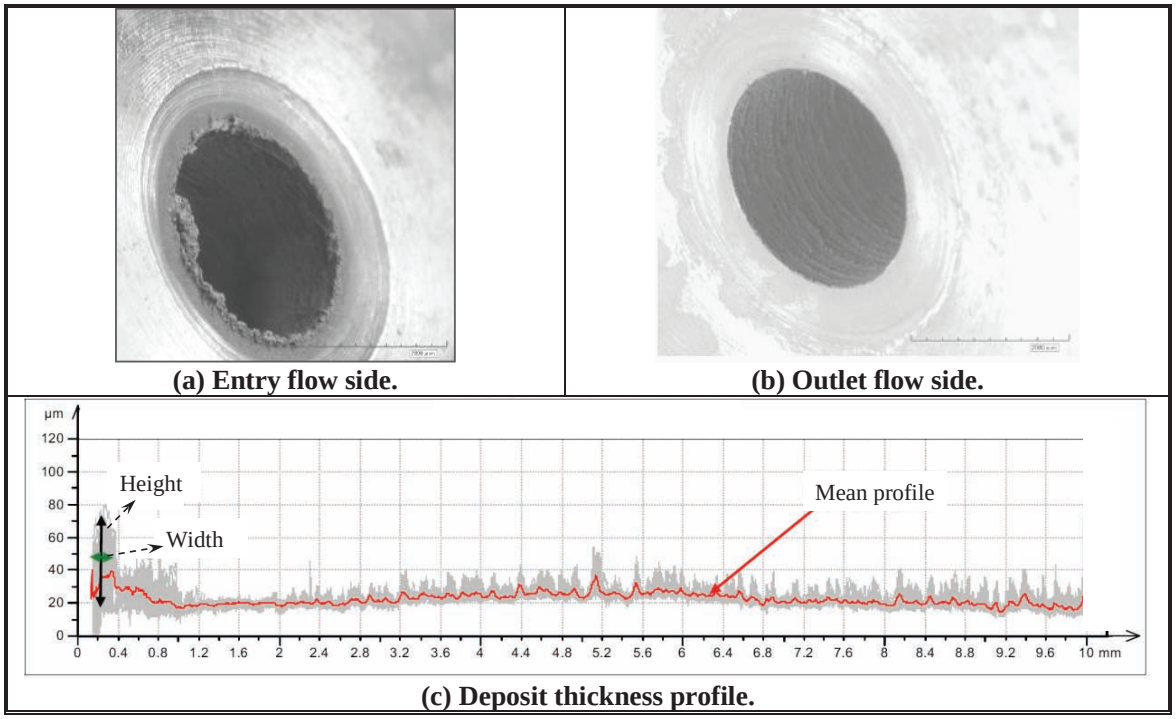

(a) Entry flow side. **(b) Outlet flow side.**

(c) Deposit thickness profile.

Figure 5 - Thickness profile 760 h into the test (low iron concentration)

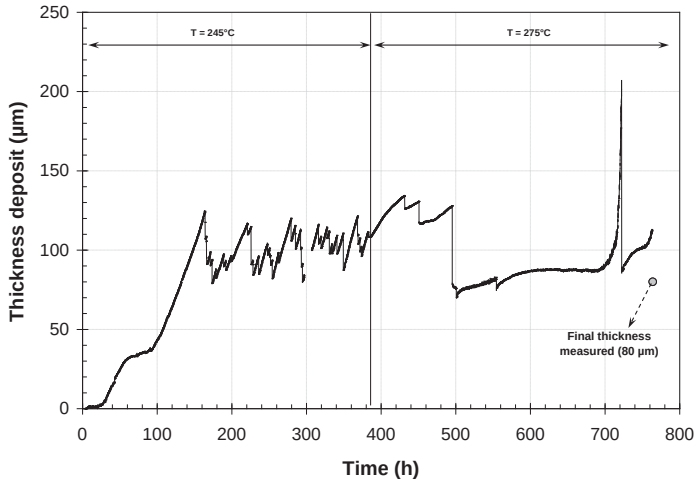

Figure 6 - Average deposit thickness as a function of test duration (low iron concentration (5 to 9.5 ppb) at 245 and 275°C)

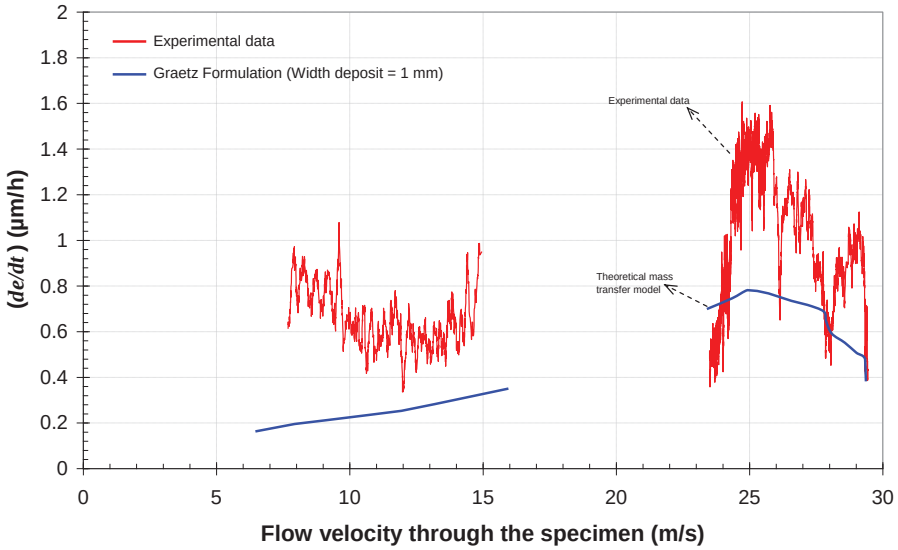

Figure 7 - Thickness growth velocity as a function of flow velocity through the specimen for experimental and theoretical estimations (low iron concentration)

Finally, the model calculation was compared with real data (on-site measurements) from a steam generator device of a nuclear power plant.

On-site, different physico-chemical and process parameters are recorded daily. We input these parameters in order to estimate the iron concentration and so to predict the clogging kinetics on the tube' support plate at the different levels along the steam generator.

The CLOSIS program was developed by AREVA in order to simulate the clogging phenomena into a steam generator at full-scale. This program takes into account the thermal-hydraulic conditions (1D modelling of a steam generator. The physico-chemical properties calculated by OLI chemical thermodynamic code (www.olisystems.com) to compute the dissolved iron concentration. The mass

transfer model showed in section 2 was implemented in CLOSIS. We assume that the deposit grows with a shape similar to the one observed on our experimental tests for on-site experience feedback. As flow velocity in full-scale is lower than in our test conditions, the deposit kinetics is much slower, and the clogging phenomena take more time (several years). Currently, the model can not estimate the lag time because the mechanism which activates the deposition is not still well understood, therefore this value is estimated from real data.

The simulation results were computed as Circulation Ratio (CR), because this factor is directly linked to pressure drop and then to the clogging of the tube' support plate. Circulation Ratio is determined by the equilibrium between driving forces (difference in density) and the pressure drops of the recirculation loop in the steam generator device. The greater the clogging, the lower the CR due to pressure drop increases.

The Figure 8 shows the good agreement between the Circulation Ratio and model prediction for 20 years of operation. In this case, the lag time phenomenon can be neglected because this value is much lower compared to simulation time.

Further validation based on other steam generators data are still necessary to validate the model; however these good results would show that the clogging phenomena in SG could be calculated by our model in order to estimate the clogging level and its impact on steam generator operating parameters and performances.

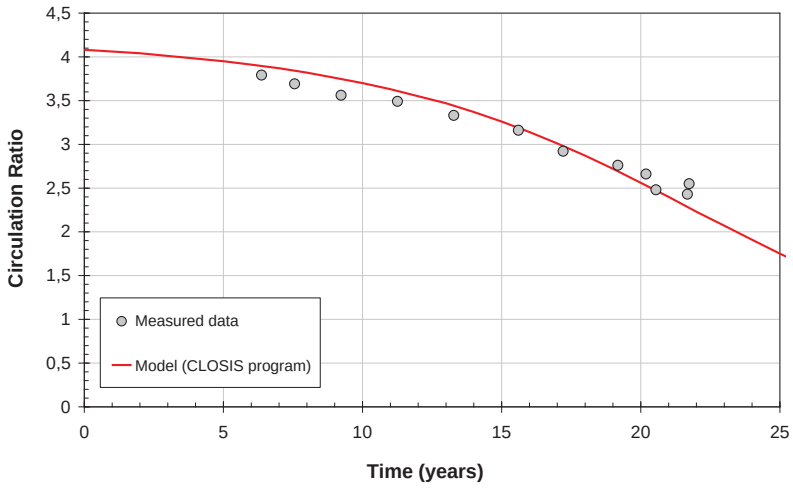

Figure 8 – Theoretical prediction and measurement of the Circulation Ratio (on-site data) of a steam generator in a nuclear power plant.

5. Conclusions

Experimental and modelling studies were performed to understand the clogging effect on the surface of a geometrical singularity. The experimental test was carried out at a temperature between 245 and 275°C and a pressure of 10 MPa, with a water velocity of 30 to 5 m.s-1 and iron concentration of 5 to 9.5 ppb for 760 hours. Tests showed a large deposit of magnetite mainly at the specimen entry with a thickness of 115 µm and 570 µm for the low and high iron concentrations respectively. In addition, a roll-deposit perpendicular to the flow direction was noticed along the entire length of the specimen.

The mean thickness of the deposit on the specimen was estimated on the basis of pressure drop coefficient calculations using deposit geometries similar to those observed at the end of our tests. A correlation model was also built to estimate the mean thickness of the deposit using mass transfer correlations (Graetz formulations).

The model and experimental results have shown a good agreement on the estimated deposit kinetics evolutions (de/dt). These results suggest that the clogging effect in our experimental conditions is controlled by mass transfer. Nevertheless, the electrokinetic effect due to streaming currents provides the initial surface conditions to produce the deposit. This important observation could greatly simplify the modelling of deposits using well known mass transfer correlations.

Finally, the model calculation was compared with real data (on-site measurements) from on-site steam generator device of a nuclear power plant (program developed by AREVA). We noticed that theoretical estimations are in agreement with on-site measurement and this for 20 years' experience feedback.

On the whole, these results show that the clogging phenomena on tubes' support plate could be predicted satisfactorily considering the Graetz mass transfer correlation and some assumptions on the clogging shape. However, further validation of the model must be carrier out with on-site data from other steam generator, and complementary studies are still necessary in order to understand the physico-chemical mechanisms generating of the deposit formation and stabilization.

Acronyms and symbols

CR	Circulation Ratio
PWR	Pressurized Water Reactor
SG	Steam Generator
TSP	Tube' Support Plates

A_n	Constant from R.H. Notter and C.A. Sleicher equations (-)
c	Parameter in asymptotic relation for A_n and C_n
C	Concentration ($kg.m^{-3}$)
D	Diameter (m)
D_m	Molecular diffusion coefficient ($m^2.s^{-1}$)
e	Deposit thickness (m) or exponential function (-)
f	Friction factor (-)
G	Dimensionless constant from R.H. Notter and C.A. Sleicher equations (-)
H	Dimensionless constant from R.H. Notter and C.A. Sleicher equations (-)
K	Pressure drop coefficient (-)
k	Redefined eigenvalue from R.H. Notter and C.A. Sleicher equations (-)
k_B	Boltzmann's constant ($J.K^{-1}$)
k_m	Mass transfer coefficient ($kg.m^{-2}.s$)
l_C	Width of deposit at the entry of the specimen (m)
N	Mass flux ($kg.m^{-2}.s^{-1}$)
P	Pressure (Pa)
P_r	Prandtl number (-)
r	Radius of the spherical particle (m)
Re	Reynolds number (-)
S	Axial area (m^2)
Sc	Schmidt number (-)
Sh	Sherwood number (-)
t	Time (s)
T	Temperature (°C)
v	Velocity ($m.s^{-1}$)
X	Dimensional axial variable (m)
x	Dimensionless axial variable (-)

Greeks symbols

α	Angle of conical diffuser (Degrees)
μ	Viscosity ($kg.m^{-1}.s^{-1}$)
π	3.14159…
ρ	Density ($kg.m^{-3}$)
ε	Roughness (m) or porosity
Δ	Gradient (-)

λ	Linear coefficient (-)
λ_n	Nth eigenvalue from R.H. Notter and C.A. Sleicher equations (-)
Subscripts	
0	Initial conditions
C	Entry specimen section with clogging
Fe	Iron
i, j, A, B, …	Different sections of the specimen

References

[1] H. Bodineau, T. Sollier, Tube support plate clogging up of French PWR steam generators, Eurosafe, Towards Convergence of Technical Nuclear Safety Practices in Europe, (www.eurosafe-forum.org) 2008.

[2] T. Prusek, Modélisation et simulations numérique du colmatage à l'échelle de sous-canal dans les générateurs de vapeur, PhD report, Ecole Doctorale Sciences Pour l'Ingénieur, Aix-Marseille Université, France, 2012.

[3] A.V. Delgado, F. Gonzalez-Caballero, R.J. Hunter, L.K ; Koopal, J. Lyklema, Measurement and interpretation of electrokinetic phenomena, Journal of Colloid and Interface Science, 309 (2007) 194-224.

[4] M. Guillodo, P. Combrade, B. dos Santos, T. Muller, G. Berthollon, N. Engler, C. Brun, G. Turluer, Formation of Deposits in HT Water under High Velocity Conditions: a Parametric Study, International conference of Water Chemistry og Nuclear Reactor Systems, 2004.

[5] M. Guillodo, M. Guingo, M. Foucault, N. Ryckelynck, F. Chahma, C. Mansour, O. Alos-Ramos, G. Corredera, Experimental and numerical study of deposit formations in secondary side SG TSP by electrokinetic approach, Nuclear Plant Chemistry Conference, 2012.

[6] C. Henry, J.-P. Minier, G. Lefèvre, Towards a description of particule fouliong: From single particle deposition to clogging, Advances in Colloid and Interface Science, 185-186 (2012) 34-36.

[7] S. Girard, T. Romary, J.-M. Favennec, P. Stabat, H. Wackernagel, Sensitivity analysis and dimension reduction of a steam generator model for clogging diagnosis, Reliability Engineering and System Safety 113 (2013) 143-153.

[8] C. Burn, N. Engler, G. Berthollon, T. Muller, B. Sala, P. Combrade, G. Turluer, Investigation on the relation between pressure drops and fluid chemical treatment. International Conference in Water Chemistry, Avignon (2002).

[9] I.S. Woosley, D.M. Thomas, K. Garbett, Occurrence and prevention of enhanced oxide deposition in boiler flow control, Water chemistry of nuclear reactor systems. London, (1988).

[10] J. Roberson, Corrosion and deposition due to electrokinetic currents. CERL note n° TPRD/L/3030/R86 (1986).

[11] I.E. Idelchik, Handbook of Hydraulic Resistance, 3rd Edition 1994.

[12] R.B. Bird, W.E. Stewart, E.N. Lightfoot, Transport phenomena, Réverté 1965.

[13] R.H. Notter, C.A. Sleicher, A solution to the turbulent Graetz problem – III, Fully development and entry region heat transfer rates, Chemical Engineering Science, Vol. 27, 1972, pp. 2073 – 2093.

[14] A. Bontemps, A. Garrigue, C. Goubier, J. Huetz, C. Marvillet, P. Mercier, R. Vidil, Echangeurs de chaleur, Intensification des échanges thermiques, Techniques de l'Ingénieur, B 2 343, 2012, 1 – 18.